frontiers | Frontiers in Materials

ORIGINAL RESEARCH
published: 25 May 2022
doi: 10.3389/fmats.2022.863305

Coarsening Evolution of γ′ Phase and Failure Mechanism of Co-Ni-Al-Ti-Based Superalloys During Isothermal Aging

Xuming Zhang[1,2], *Hang Shang*[1,2], *Qiuzhi Gao*[1,2]*, *Qingshuang Ma*[1,2], *Hailian Zhang*[3]*, *Huijun Li*[4] and *Linlin Sun*[1,2]

[1]School of Materials Science and Engineering, Northeastern University, Shenyang, China, [2]School of Resources and Materials, Northeastern University at Qinhuangdao, Qinhuangdao, China, [3]Daotian High Technology Co., Ltd., Qinhuangdao, China, [4]School of Mechanical, Materials and Mechatronic Engineering, University of Wollongong, Wollongong, NSW, Australia

Novel Co-based superalloys, as potentially ideal aero-engine hot section materials, have a higher temperature bearing capacity and better oxidation resistance than Ni-based superalloys. Coarsening evolution of γ′ phase and failure mechanism of Co-Ni-Al-Ti-based superalloys during the isothermal aging process at 1073 K were investigated using multiple characterizations and testing methods. The results show that γ′ phase is uniformly distributed on the γ phase matrix, and coarsening with the increase in isothermal aging time, which results in a decrease in maximum tensile strength. Furthermore, Mo element is preferred to distribute in γ′ phase and provides stronger solution strengthening effect than Cr element, which determines more excellent mechanical properties of 2Mo superalloy than that of 2Cr superalloy. The coarsening rate of γ′ phase in the 2Cr superalloy is significantly higher than that in the 2Mo superalloy. Grain boundary failure is dominant in isothermal aging, and the cracks nucleate and expand along the vertical direction of loading stress on the grain boundary. The current work suggests that the coarsening of the γ′ phase, reduction in the volume fraction of γ′ phase, and formation of ′-precipitate depleted zone (PDZ) near the grain boundary during aging controls the deterioration of mechanical properties in Co-Ni-Al-Ti-based superalloys.

Keywords: Co-Ni-Al-Ti-based superalloy, γ′ phase, coarsening rate, isothermal aging, mechanical properties

OPEN ACCESS

Edited by:
Wei-Wei Xu,
Xiamen University, China

Reviewed by:
Qing Wang,
Dalian University of Technology, China
Yilu Zhao,
Harbin Institute of Technology, China

***Correspondence:**
Qiuzhi Gao
neuqgao@163.com
Hailian Zhang
hailianchina@126.com

Specialty section:
This article was submitted to Structural Materials, a section of the journal Frontiers in Materials

Received: *27 January 2022*
Accepted: *19 April 2022*
Published: *25 May 2022*

Citation:
Zhang X, Shang H, Gao Q, Ma Q, Zhang H, Li H and Sun L (2022) Coarsening Evolution of γ′ Phase and Failure Mechanism of Co-Ni-Al-Ti-Based Superalloys During Isothermal Aging. Front. Mater. 9:863305. doi: 10.3389/fmats.2022.863305

INTRODUCTION

Superalloys, as key structural materials in the aerospace field, have been widely used in aerospace engines and gas turbines (Jiang et al., 2020; Gao et al., 2021a; Gao et al., 2021b; Gao et al., 2022). Beforehand, Ni-based superalloys are the most successfully applied superalloys in this field (Pandey et al., 2021). Due to the not quite high melting point, improvement in the high temperature bearing capacity of Ni-based superalloys is severely restricted (Gao et al., 2021c; Xu et al., 2021a; Xu et al., 2021b). Traditional Co-based superalloys are dependent on solution strengthening and carbide strengthening, and lack of ordered $L1_2$-γ′ phase precipitation strengthening widely present in Ni-based superalloys, which results in poor mechanical properties at high temperatures (Feng et al., 2021; Lu et al., 2021). Until 2006, when Sato et al. (2006) first reported the discovery of novel Co-Al-W-based superalloys with ordered $L1_2$-γ′ phase strengthening. The higher melting point, better oxidation resistance, and mechanical

properties of novel Co-based superalloys have been proven against that of Ni-based superalloys (Zhou et al., 2020; Chen Z. et al., 2021).

Whereas the high content of W addition in the Co-Al-W superalloy leads to a relatively high density and makes it impractical to apply in the aerospace field (Singh et al., 2021). Therefore, W-free novel Co-based superalloys with order γ′ phase, such as γ′-Co_3Al (Omori et al., 2006), γ′-Co_3Ti (Zenk et al., 2017; Yoo et al., 2019), and γ′-Co_3Ta (Wang et al., 2019; Chen et al., 2020), have been rapidly developed in recent years. Guan et al. (2020a) studied the microstructure and mechanical properties of CoNi-based superalloys after being aged, and concluded that the addition of Ni, Ti, Ta elements improved the stability of the γ′ phase. Nevertheless, the high temperature stability of the γ′ phase in W-free novel Co-based superalloys is an urgent problem. Liu et al. (2019) reported that the addition of Mo reduces the yield strength of a superalloy because the Mo element leads to the precipitation of μ phase in Co-based superalloy, which reduces the mechanical properties of the superalloy. However, Zhou et al. (2018) proposed that the addition of the Mo element can change interfacial energy, thus reducing the coarsening rate of the γ′ phase, and improving the high temperature stability of superalloys. In addition, Cr elements prefer to be distributed in the γ phase matrix (Chung et al., 2020), and a large amount of Cr can reduce the volume fraction of γ′ phase in superalloys, although it can greatly improve oxidation resistance of superalloys (Chen et al., 2019; Chung et al., 2020; Li W. et al., 2020). By studying the microstructure of superalloys with different Cr contents, Ng et al. (2020) showed that higher Cr content leads to precipitation of harmful μ phase and deteriorates the mechanical properties of superalloys. In order to obtain excellent high-temperature stability and high-temperature mechanical properties, the evolution of the γ/γ′ phase in Co-based superalloys has been extensively studied (Zhou et al., 2018; Liu et al., 2019; Li C. et al., 2020). It has been reported that during the isothermal aging process of Co-based superalloys, the volume fraction of the γ′ phase will increase to a certain value and then plateau, the number density of the γ′ phase will decrease, and the size of the γ′ phase will increase (Sauza et al., 2019b; Li C. et al., 2020; Chen J. et al., 2021). Azzam et al. (2018) found that the cubic γ′ phase precipitated in Co-9.1Al-7W at% superalloys transformed into elongated colonies after aging at 900°C for 100 h. Chen J. et al. (2021) studied the γ′ coarsening behavior by phase-field simulation, and believed that ahigher volume fraction of the γ′ phase increased the chemical potential difference between the precipitated phase and matrix phase, resulting in a larger coarsening rate constant of the γ′ phase. Sauza et al. (2019a) also found the γ′ phase coarsening during the isothermal aging process of Co-Al-W-Ni superalloy, and confirmed that it conforms to Lifshitz-Slyozov-Wagner (LSW) coarsening model. Guan et al. (2022) studied the deformation behavior of CoNi-based superalloys with different heat treatment methods and found that with increasing temperature, the deformation mechanism gradually transitioned into the dislocation bypassing accompanied with the superlattice intrinsic stacking faults (SISFs) shear. The grain boundary and γ/γ′ two phase boundary are locations of crack nucleation and propagation in Co-based superalloys under stress (Wen et al., 2020). Some researchers (Guan et al., 2020b) suggest that the addition of Ni and Ti increases the coarsening rate of the γ′ phase, but the effect of Cr and Mo on γ′ coarsening during isothermal aging and the effect of γ′ coarsening on the failure mechanism of Co-based superalloys have not been reported. Hence, the study of the coarsening evolution of the γ′ precipitates and the failure mechanism in novel Co-based superalloys is necessary for better superalloy design and its performance optimization.

In this work, two Co-Ni-Al-Ti-based superalloys with Cr or Mo addition were isothermal aged at 1073 K with different holding times to investigate the microstructure evolution and mechanical properties. The effects of Cr and Mo on the microstructure evolution of Co-Ni-Al-Ti-based superalloys were studied by scanning electron microscope (SEM), X-ray diffractometer (XRD), and transmission electron microscope (TEM). In addition, the temporal exponent of the γ′ phase coarsening process and diffusion coefficients of Cr and Mo in FCC-Co were calculated, and effect mechanisms of Cr and Mo elements on the γ′ phase coarsening rate of two Co-Ni-Al-Ti-based superalloys were also discussed.

MATERIALS AND METHODS

The Co-Ni-Al-Ti-based superalloys used in this study were prepared by mixing and melting high purity metals including Co. (99.95wt%), Ni (99.8wt%), Al (99.95wt%), Ti (99.95wt%), Cr (99.8wt%), and Mo (99.95wt%) in a vacuum induction furnace. Each ingot was inverted and re-melted 6 times to ensure homogeneity, and subsequently measured using Inductive Coupled Plasma-Optical Emission Spectrometry (ICP-OES). The nominal and actual compositions of superalloys are shown in **Table 1**, and named as 2Cr and 2Mo. Melted ingots were homogenized at 1473 K for 4 h, and rolled into plates with a thickness of 12 mm at 1423 K. The samples were cut by electro-discharge machining and isothermal aging for 16, 64, 256, and 512 h at 1073 K in a Muffle furnace, respectively. In addition, Differential Scanning Calorimetry (DSC) was also applied to measure the γ′ phase solvus temperature with the aim to analyze the effect of aging temperature on the volume fraction of the γ′ phase, and the obtained results were also listed in **Table 1**.

Isothermal aged samples were polished to a mirror surface on a series of SiC paper, and then etched in 10% phosphoric acid solution to observe the γ′ phase by scanning electron microscope (SEM). X-ray diffraction (XRD) was performed using a diffractometer equipped with Cu Kα radiation (λ = 0.154056 nm), and lattice misfit was calculated by XRD results. A scanning range of 2θ degrees was set from 20° to 100° with a scanning rate of 4°/min. The diffraction peak (111) is used for peak fitting and lattice misfit calculation because the peak (111) has sufficient strength. The microstructure of superalloys was characterized by scanning electron microscope (SEM, ZEISS

TABLE 1 | Chemical compositions (at%) and γ′ solvus temperature (K) of 2Cr and 2Mo superalloys.

Superalloys	γ′ solvus temperature (K)		Composition (at%)					
			Co	Ni	Al	Ti	Cr	Mo
2Cr	1128	Nominal	Bal	30.00	7.50	2.50	2.00	-
		Actual	Bal	29.86	7.34	2.54	2.03	-
2Mo	1162	Nominal	Bal	30.00	7.50	2.50	-	2.00
		Actual	Bal	29.15	7.53	2.54	-	2.01

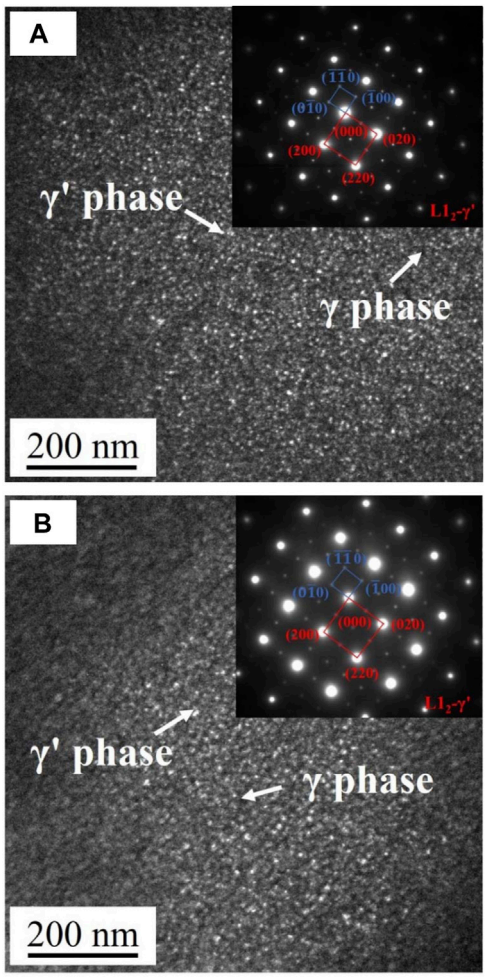

FIGURE 1 | Hot-rolled TEM micrographs of Co-Ni-Al-Ti-based superalloys: **(A)** 2Cr, **(B)** 2Mo.

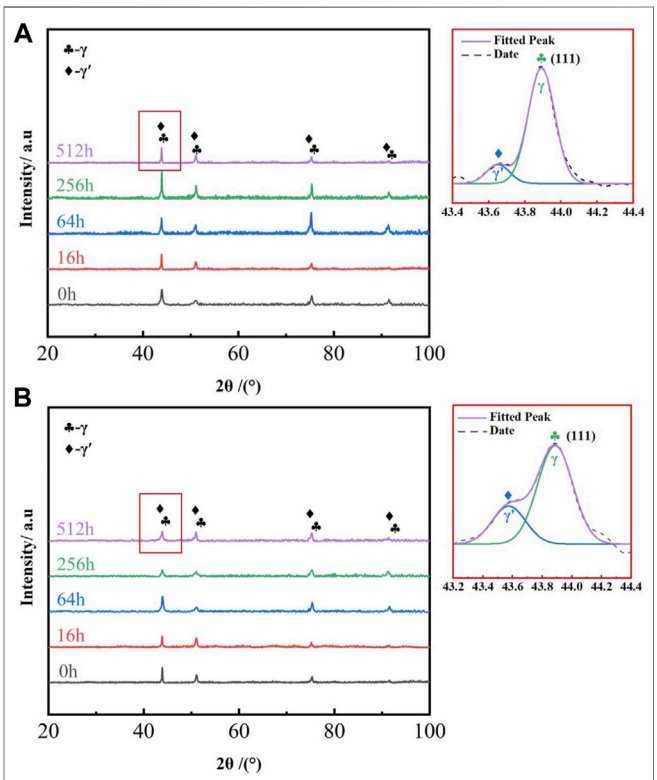

FIGURE 2 | XRD patterns of hot-rolled samples and after aging at 1073 K: **(A)** 2Cr, **(B)** 2Mo.

SUPRA 55) and transmission electron microscope (TEM). The TEM samples were polished to a mirror surface using SiC paper and perforated into 3 mm diameter holes, and the ion erosion was used to further reduce sample thickness. The volume fraction and size of γ′ phase in superalloys were analyzed by Image Pro software on 20 SEM micrographs.

Vicker's hardness was tested with a load of 5 Kg for 5 s, the final result for each sample was the average value of ten measurements, and standard deviation of these measurements was taken as error. Meanwhile, a tensile test at room temperature was conducted with dog-bone plate tensile samples with gauge length of 10 mm and a loading initial strain rate of 2 mm/min. Before the tensile test, all surfaces of samples had been polished smooth with SiC paper, and elongation of the specimen was measured manually.

RESULTS

Microstructural Evolution During Isothermal Aging

Figure 1 shows the hot-rolled TEM micrographs of two Co-Ni-Al-Ti-based superalloys, the white fine γ′ phase and γ phase matrix can be observed, and were further identified from selected area electron diffraction (SAED) patterns. The SAED pattern

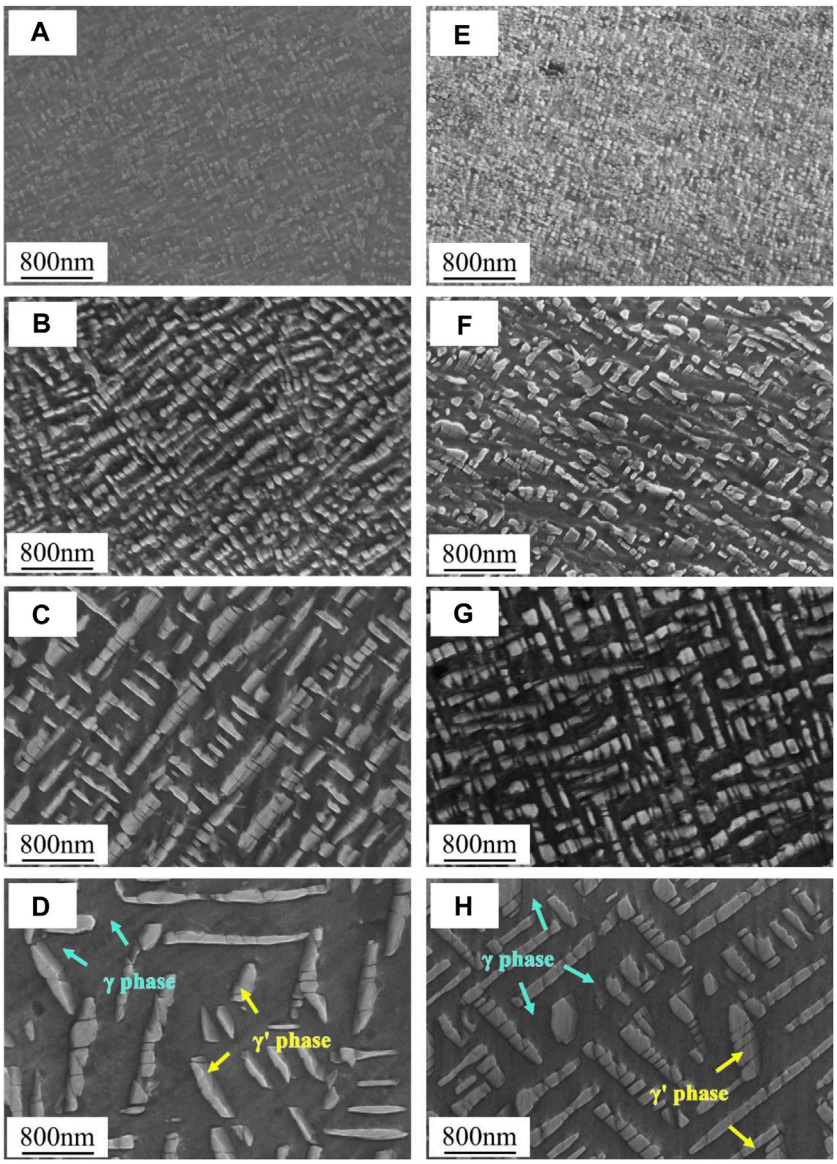

FIGURE 3 | SEM micrographs of typical microstructures in Co-Ni-Al-Ti-based superalloys: **(A–D)** 2Cr for 16, 64, 256, and 512 h, and **(E–H)** 2Mo for 16, 64, 256, and 512 h at 1073 K.

shows that the crystal planes of the γ′ phases are parallel to the γ phases respectively, which indicates that γ/γ′ phases are coherent in hot-rolled samples. In addition, XRD patterns of hot-rolled and isothermal aged samples are shown in **Figure 2**. The X-ray incident angle corresponding to each diffraction peak in XRD patterns have little difference in aged samples and hot-rolled samples. Similar lattice structures and lattice parameters are bases for the formation of coherent interfaces. By comparing the XRD patterns of all specimens, the almost overlapping γ′ phase and γ phase diffraction peaks confirmed the coherent relation is not destroyed in the isothermal aging process (Yoo et al., 2019; Chen et al., 2020; Chung et al., 2020). The phase boundary between γ matrix phase and γ′ precipitated phase is a coherent phase boundary, which plays a certain strengthening role for mechanical properties in superalloys. There are no diffraction peaks for other phases.

SEM micrographs of Co-Ni-Al-Ti-based superalloys after isothermal aging at 1073 K with different times are shown in **Figure 3**. Only the white $L1_2$-γ′ phase dispersed on the γ matrix can be observed in isothermal aged samples. The morphology of the γ′ phase in superalloys is driven by elastic energy and interfacial energy, in which elastic energy is anisotropic and interfacial energy is isotropic (Chen J. et al., 2021). Hence, the morphology of the γ′ phase may be controlled by a change of lattice misfit during isothermal aging. Besides, with an increase in isothermal aging time, the γ′ phase is obviously coarsened, which is harmful to the high temperature strength and stability of the superalloys. Meanwhile, it can be observed that with an extension

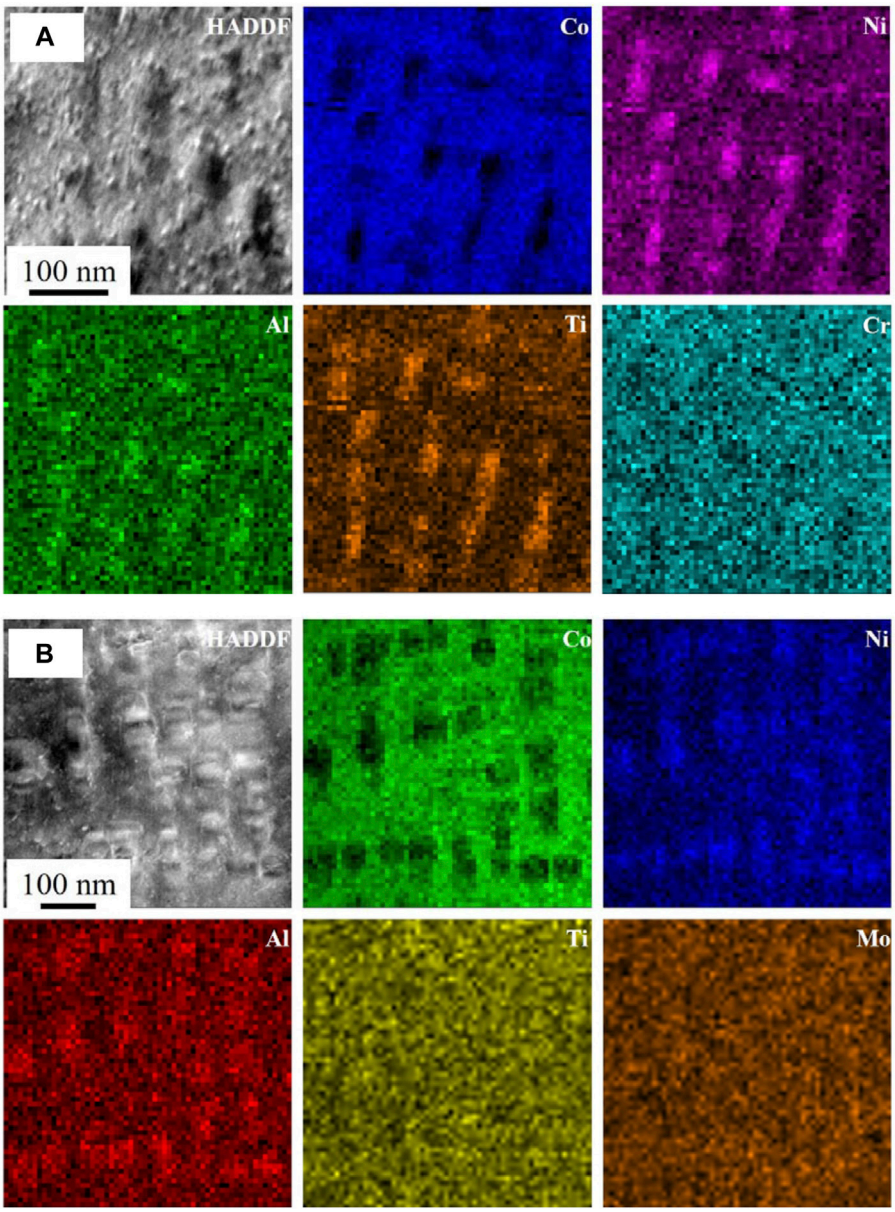

FIGURE 4 | The high-angle annular dark field (HAADF) images in the [1 0 0] zone axis and elemental mapping for the cuboidal precipitates using a TEM nanoprobe of superalloys aged at 1073 K for 32 h: **(A)** 2Cr, and **(B)** 2Mo.

of the isothermal aging time, the number of γ′ phases is decreased gradually, due to the connection between γ′ phases. The HAADF images in the [1 0 0] zone axis and elemental mapping for cuboidal precipitates of superalloys isothermally aged 32 h at 1073 K are shown in **Figure 4**. The results show that Co prefers to be distributed in the γ phase matrix, while Ni, Al, and Ti can be observed in the γ′ phase. Cr tends to be distributed in the γ phase matrix, while Mo is enriched in the γ′ phase but not obviously, which is consistent with results of other references (Yoo et al., 2019; Chen et al., 2020). Therefore, $(Co, Ni)_3$ (Al, Ti) can be confirmed as the component of the precipitated $L1_2$-γ′ phase in current Co-Ni-Al-Ti-based superalloys, *i.e.*, γ′-$(Co, Ni)_3$ (Al, Ti) formed.

The average size of γ′ phase in two superalloys after isothermal aging are shown in **Figure 5A**, and it gradually increases with the prolongation of the isothermal aging time. In the isothermal aging process of Co-Ni-Al-Ti-based superalloys, the growth of the γ′ phase consists of two stages: the first stage, which depends on the diffusion of solute atoms, and the second stage, which depends on merger of the γ′ phase (Ng et al., 2020). The average size of the γ′ phase in two Co-Ni-Al-Ti-based superalloys are similar during a short isothermal aging time, however, in 2Cr, it is

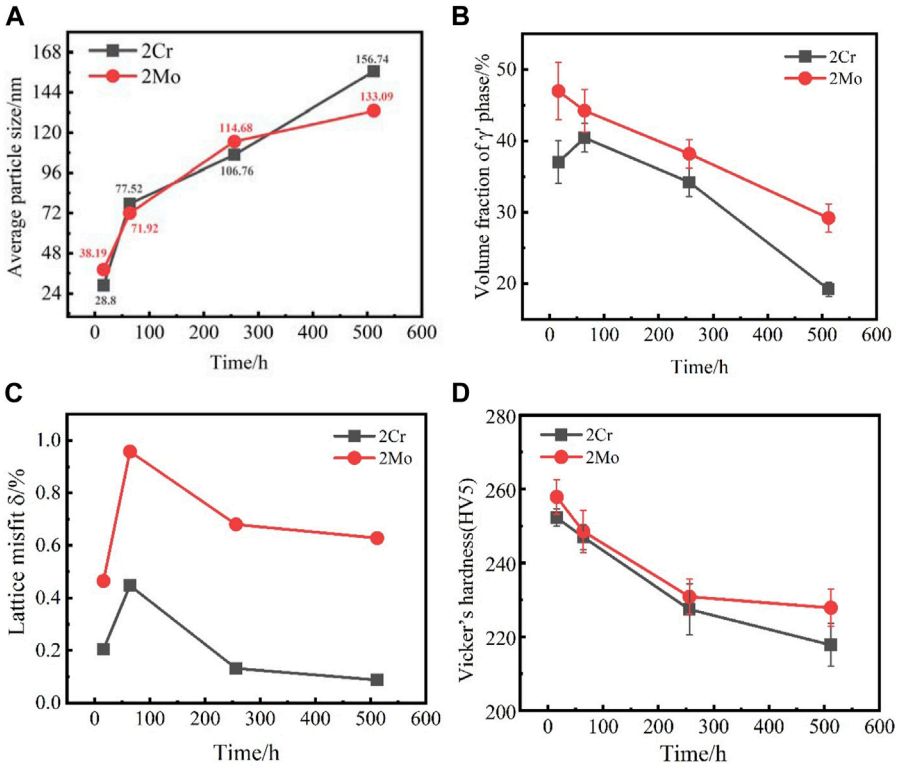

FIGURE 5 | The average size of the γ′ phase and lattice misfit of 2Cr and 2Mo superalloys after aging at 1073 K: **(A)** the average size of the γ′ phase, **(B)** volume fraction of the γ′ phase, **(C)** lattice misfit, and **(D)** Vicker's hardness.

obviously larger than in 2Mo after a long time of isothermal aging. It is confirmed that the coarsening rate of the γ′ phase in the 2Cr superalloy is higher than that in the 2Mo superalloy after a long time aging. The volume fraction of the ′ phase during isothermal aging is shown in **Figure 5B**. With aging time increasing, the content of the γ′ phase gradually decreases. This may be caused by high aging temperature (1073 K), because the γ′ phase solvus temperatures of 2Cr and 2Mo superalloys are 1128 and 1162 K as shown in **Table 1**, respectively, and the aging temperatures are only lower by 55 and 89 K than the measured γ′ solvus temperature. Part of the γ′ phases dissolves when the samples are aged for a long time at a higher temperature. In addition, similar results have been found in other cases (Zhou et al., 2018; Gao et al., 2020). It is worth noting that the volume fraction of the γ′ phase in 2Mo (29.2 ± 2%) is higher than that in 2Cr (19.2 ± 1%) which was isothermally aged for 512 h, which may be due to Mo being more strongly allocated to the γ′ phase than Cr (Zhang et al., 2018; Zhuang et al., 2020).

In order to discuss the effect of alloying elements on the morphology of the γ′ phase and mechanical properties of superalloys, the peak profiles of XRD patterns were approximated by Voigt distribution function, and lattice parameters of the γ′ phase and γ phase were determined (Mukherji et al., 2003; Chen et al., 2020). The lattice misfit is defined as:

$$\delta = 2 \times \frac{\alpha_{\gamma'} - \alpha_{\gamma}}{\alpha_{\gamma'} + \alpha_{\gamma}} \tag{1}$$

where $\alpha_{\gamma'}$ and $\alpha_{\gamma'}$ are lattice parameters of the γ′ phase and γ matrix phase respectively. The Bragg equation was used to calculate lattice parameters of the γ′ phase and γ matrix phase, and assuming cubic symmetry from location of the peaks in diffraction angle 2θ. The following formula is obtained:

$$\alpha = \frac{\lambda\sqrt{h^2 + k^2 + l^2}}{2\sin\theta} \tag{2}$$

where λ is the wavelength of X-rays used (in this experiment, λ = 0.154056 nm), and (*h, k, l*) is Miller indices of lattice plane under investigation.

The Voigt function was used to fit and separate the (111) diffraction peaks of superalloys after isothermal aging, meanwhile the lattice parameters of the γ′ phase and γ matrix phase and lattice misfit of superalloys was calculated by the above equations. **Figure 5C** shows that the lattice misfit of γ′/γ two phases in 2Cr and 2Mo superalloys after different amounts of time spent isothermal aging. With the increase in isothermal aging time, the lattice misfit of two Co-Ni-Al-Ti-based superalloys increases first and then decreases. First, alloying elements diffuse to the γ′ phase the leads to an increase of lattice misfit of the $L1_2$-γ′ phase at the early aging stage. However, with the extension of aging time, the γ/γ′ interface tends to be stable and the lattice strain and

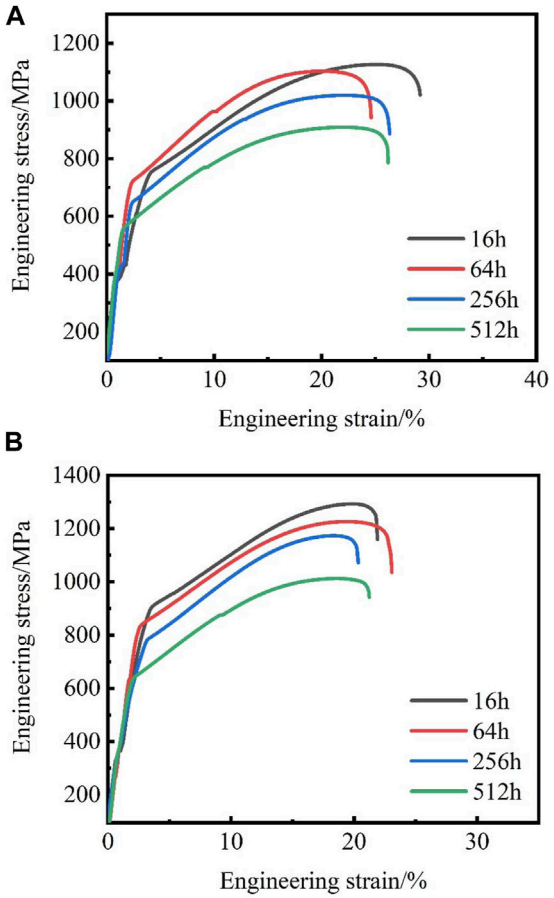

FIGURE 6 | Stress-strain curves of Co-based superalloys at room temperature: **(A)** 2Cr, **(B)** 2Mo.

TABLE 2 | Tensile properties of 2Cr and 2Mo superalloys aged samples.

Aging time (h)	2Cr			2Mo		
	UTS/MPa	YS/Mpa	ε/%	UTS/Mpa	YS/Mpa	ε/%
16 h	1127	755	29.2	1293	909	21.9
64 h	1102	721	24.6	1226	842	23.1
256 h	1019	653	26.3	1173	784	20.3
512 h	909	556	26.2	1012	643	21.2

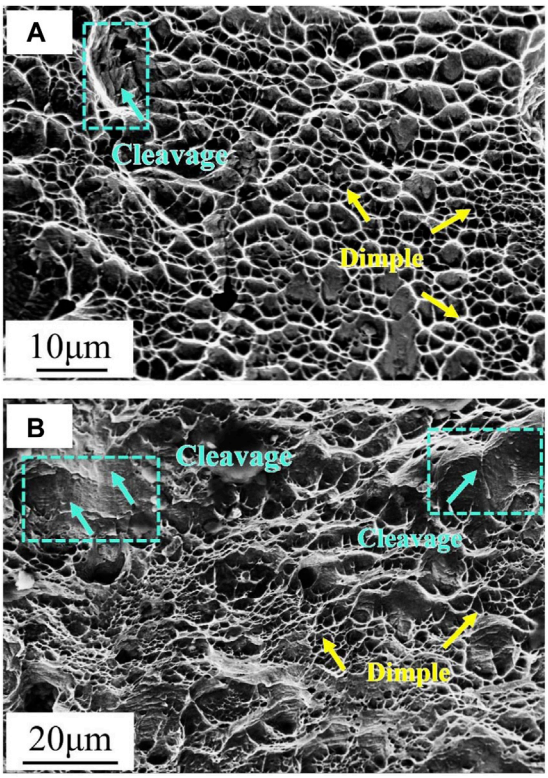

FIGURE 7 | Tensile fracture surfaces of superalloys at room temperature after being aged for 64 h at 1073 K: **(A)** 2Cr, **(B)** 2Mo.

lattice misfit decrease gradually. However, it is interesting that the lattice misfit of the 2Mo superalloy is larger than that of the 2Cr superalloy. This is because of the larger radius of the Mo atom compared to that of the Cr atom, so larger lattice distortion is caused by atoms doped into $L1_2$-γ′ lattice, in addition to Mo and Cr tending to be distributed in the γ′ phase and γ matrix phase respectively (Gao et al., 2020). Although higher lattice misfit can effectively hinder the movement of dislocations during superalloy deformation and improve mechanical properties of superalloys (Zenk et al., 2014), the coarsening of the γ′ phase also negatively affects the mechanical properties of superalloys.

Mechanical Properties

Figure 5D shows Vicker's hardness of two Co-Ni-Al-Ti-based superalloys after isothermal aging. The Vicker's hardness of 2Cr and 2Mo decreased from 252.2 N/mm^2 and 257.8 N/mm^2 to 217.8 N/mm^2 and 227.8 N/mm^2 respectively, from 16 to 512 h of aging time. The hardness of two superalloys decreases with the increase of isothermal aging time, which is caused by the decrease of volume fraction and the coarsening of the γ′ phase. The hardness of the 2Mo superalloy is higher than that of the 2Cr superalloy due to the higher volume fraction of the γ′ phase. In addition, the solution strengthening constant can reflect the strength of the solution strengthening effect of alloying elements in a superalloy. The larger the solid solution strengthening constant of an alloying element, the stronger the solid solution strengthening effect on the element. The solid solution strengthening constant of Mo element 1015 [MPa (at. fraction$^{-1/2}$)] is much larger than that of Cr element 337 [MPa (at. fraction$^{-1/2}$)], so the Mo element has a stronger solid solution strengthening effect on the superalloy (Zhang et al., 2018; Gao et al., 2020).

Figure 6 shows the engineering stress-strain curves of the 2Cr and 2Mo superalloys, and the tensile properties are presented in **Table 2**. Interestingly, the strength of two superalloys showed a similar trend to vicker's hardness with isothermal aging time. It can be found that both the ultimate tensile strength (UTS) and yield strength (YS) of 2Cr and 2Mo superalloys gradually decrease with an

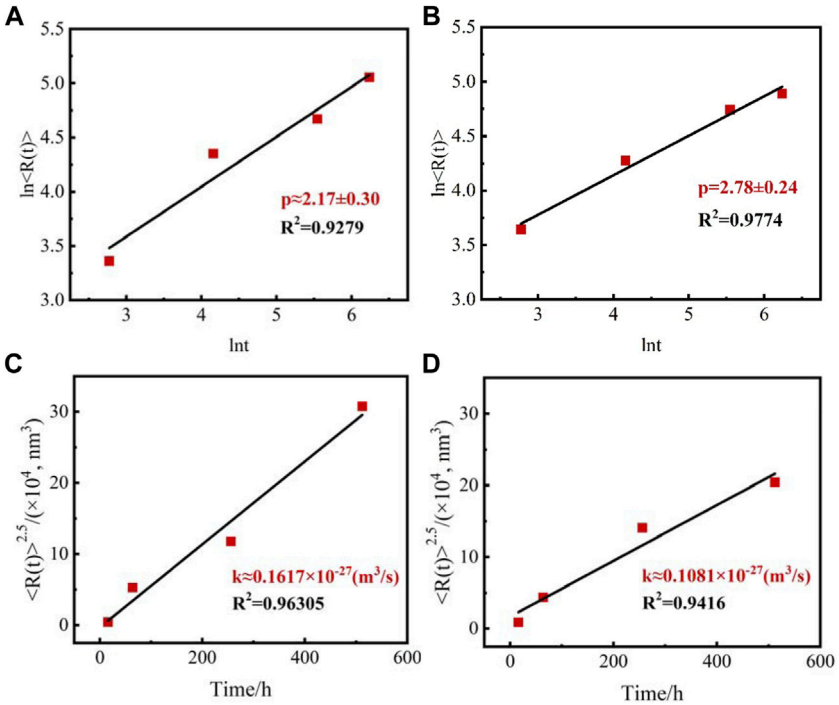

FIGURE 8 | The plot of $\ln R_{(t)}$ as a function of ln*t* during aging at 1073 K, and the 2.5 power of the mean precipitate radius $[R_{(t)}^{2.5}]$ vs. aging time (*t*) during aging at 1073 K: **(A,C)** 2Cr, **(B,D)** 2Mo.

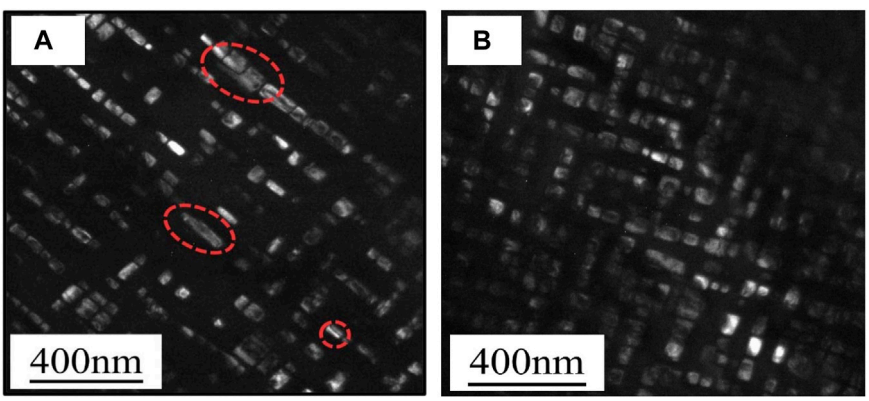

FIGURE 9 | The TEM micrographs of typical microstructures in superalloys after being aged for 32 h at 1073 K: **(A)** 2Cr, **(B)** 2Mo.

increase in isothermal aging time. In the 2Cr superalloy, the UTS and YS decrease from 1127 MPa to 755 MPa aged 16 h to 909 MPa and 556 MPa aged 512 h respectively. Meanwhile, in the 2Mo superalloy, the UTS and YS decrease from 1293 MPa to 909 MPa aged 16 h to 1012 MPa and 643 MPa aged 512 h respectively. This is because of the sharp coarsening of the γ′ phase and reduction in the volume fraction of the γ′ phase during isothermal aging process of superalloys. In addition, it can be found that the UTS and YS of the 2Mo superalloy are higher than those of the 2Cr superalloy, which is ascribed to the following two reasons: 1) As a solute atom, Mo causes local lattice distortion in superalloys, which increases resistance of dislocation movement and makes it difficult to dislocate or slip (Gao et al., 2020); 2) Mo prefer to be distributed in the γ′ phase compared to Cr, which increases the volume fraction of the γ′ phase in the 2Mo superalloy, and strengthens the mechanical properties of the 2Mo superalloy (Makineni et al., 2015b; Chung et al., 2020).

Figure 7 shows the SEM micrographs of tensile fracture at room temperature of two Co-Ni-Al-Ti-based superalloys aged at 1073 K for 64 h. There are a lot of dimples on fracture surface of the 2Cr superalloy, as shown in **Figure 7A**. Whereas, for the 2Mo superalloy, in addition to some dimples, relatively smooth

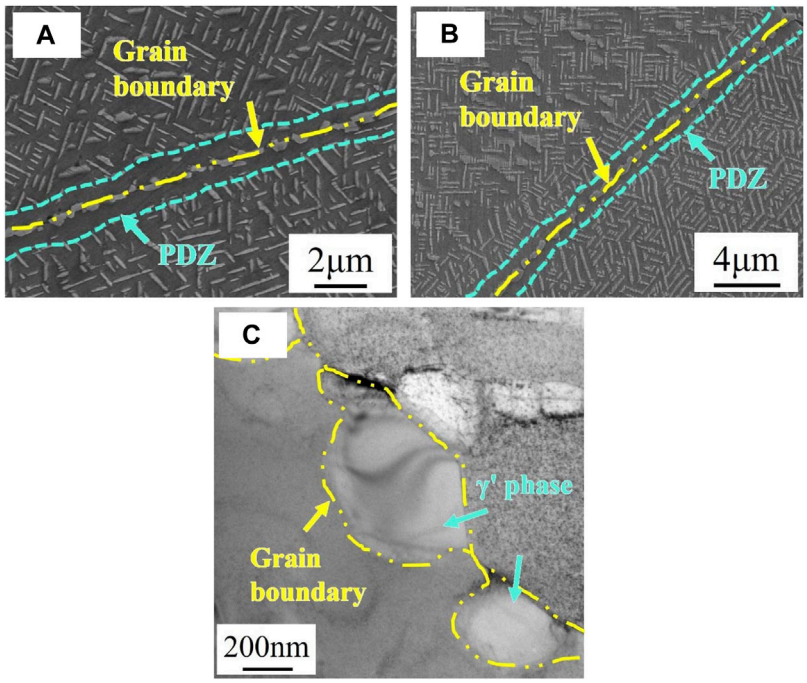

FIGURE 10 | SEM and TEM micrographs of superalloys aged at 1073 K: **(A)** 2Cr for 512 h, **(B)** 2Mo for 512 h, and **(C)** 2Mo for 32 h.

TABLE 3 | Frequency factorD_0, diffusion activation energy Q and diffusion coefficient D_1 of Cr and Mo atoms in FCC-Co at 1073 K (Neumeier et al., 2016).

Alloying elements	D_0/(m^2/s)	Q/(kJ/mol)	D_1/(m^2/s)
Cr	9.8×10^{-6}	255.4	3.61×10^{-18}
Mo	2.0×10^{-5}	262.0	3.51×10^{-18}

cleavage surfaces can also be observed on the fracture surface, as shown in **Figure 7B**. In two-phase materials (with different hardnesses), stress concentration also occurred at the interface due to a strain mismatch between the two phases, resulting in the nucleation and growth of holes. Dimples are microscopic cavities produced by plastic deformation of materials in a small range, which are formed after nucleation, growth, and aggregation, and are generally considered to be the symbol of plastic fracture. Therefore, this is the reason why the elongation of the 2Mo superalloy is lower than that of 2Cr superalloy.

DISCUSSION

Coarsening Evolution of γ′ Phase

According to **Figure 6**, the coarsening of the γ′ phase in the isothermal aging process results in a decrease of mechanical properties. However, a decrease of energy in the whole system drives γ′ phase coarsening (Zhang et al., 2020). Although the establishment of traditional LSW theory adopts the following assumptions: 1) the volume fraction of the precipitated phase is low; 2) the diffusion of solute atoms in the matrix is close to zero; 3) there is no interaction between the precipitated phase and precipitated phase; 4) the stable coarsening process of the precipitated phase (Zhang et al., 2020), a lot of papers show that the LSW theory is still suitable for the calculation of γ′ coarsening in novel Co-based superalloys (Zhou et al., 2018; Sauza et al., 2019b; Li C. et al., 2020). The expression of the LSW theory is shown as follows (Jiang et al., 2019; Guan et al., 2020b; Li C. et al., 2020):

$$R^P_{(t)} - R^P_{(t_0)} = \mathrm{k}t \tag{3}$$

where $R_{(t)}$ represents the instantaneous radius of the precipitated phase, p represents the temporal exponent, $R_{(t0)}$ represents the initial radius of the precipitated phase, and k represents the coarsening rate constant. The temporal exponent $p = 3$ in the system where diffusion of solute atoms limits the coarsening of the γ′ phase, and $p = 2$ in system where the interfacial reaction limits the coarsening of the γ’ phase (Sauza et al., 2019b).

It is generally judged whether the coarsening of the γ′ phase belongs to the stable state coarsening stage by the evolution of the volume fraction of the γ′ phase, and it is considered that the steady coarsening stage is reached when the volume fraction of the γ′ phase hardly changes at all. It is found that the volume fraction of the γ′ phase does not increase after being aged for 16 h, indicating that the coarsening of the γ′ phase has reached the stable coarsening stage. Thus, the LSW theory was used to study the coarsening process of the γ′ phase in this work, even though the volume fraction of the γ′ phase decreases, ln$R_{(t)}$ and ln$t$ were

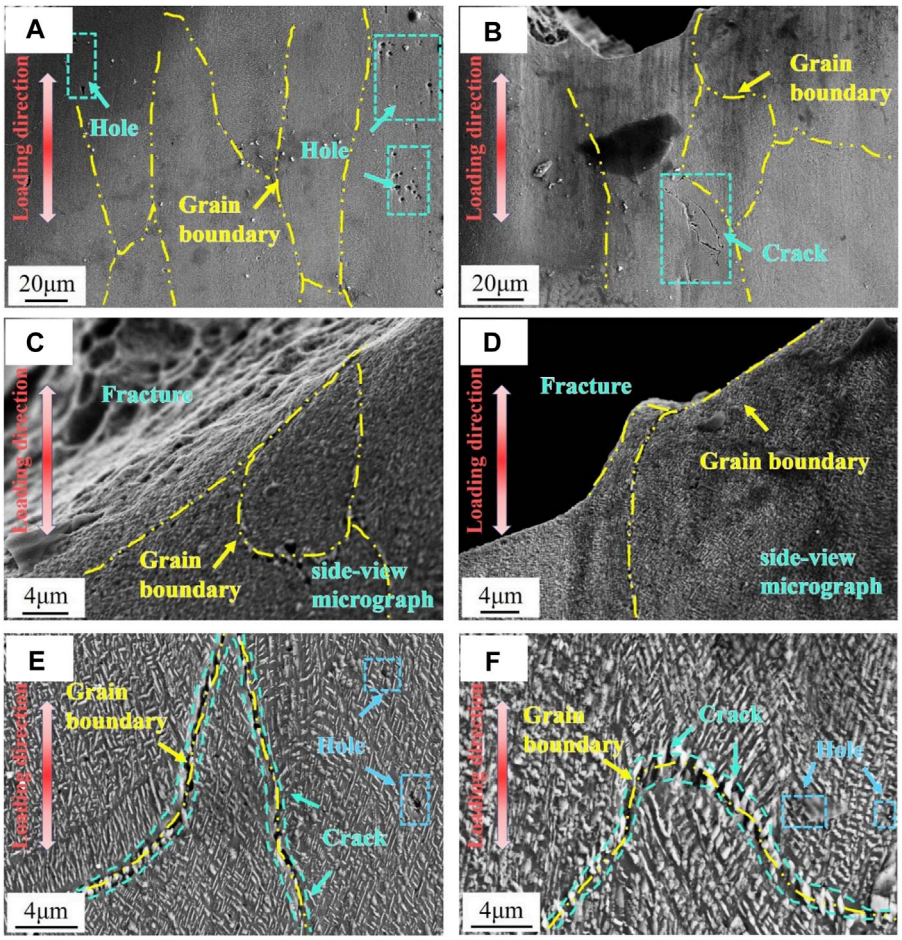

FIGURE 11 | The side-view micrographs of superalloy tensile test samples after aging at 1073 K for 512 h: **(A,C,E)** 2Cr and **(B,D,F)** 2Mo.

linearly fitted, and the results are shown in **Figures 8A,B**. It should be noted that in the 2Mo superalloy $p \approx 3$, indicating that the diffusion of solute atoms is one of the reasons for the limited γ′ phase coarsening in the 2Mo superalloy, while in the 2Cr superalloy $p = 2.17 \pm 0.24$, suggesting that interfacial reaction has a stronger limiting effect on the γ′ phase coarsening in the 2Cr superalloy (Sauza et al., 2019b; Li C. et al., 2020). By fitting the linear relationship between $R_{(t)}^{2.5}$ and t, the slope of the line can approximate the coarsening rate of the γ′ phase in Co-Ni-Al-Ti-based superalloys, 0.1617×10^{-27} m^3/s for 2Cr and 0.1081×10^{-27} m^3/s for 2Mo, as shown in **Figures 8C,D**. The coarsening rate of 2Cr is higher than that of 2Mo, but lower than Co-Ni-Al-W-Mo-Ta-Ti-based superalloys at 1273 and 1023 K reported by Zhang et al. (2020) It is similar to the coarsening rate constant of Co-Al-W-Ti-B-based superalloys aged 16–256 h at 1173 K reported by Sauza et al. (2019b), and the K value of 2Cr and 2Mo are lower than that of the Ni-based superalloys (CMSX-4, 6.86×10^{-27} m^3/s) (Lapin et al., 2008). The gap of the coarsening rate between the 2Cr superalloy and 2Mo superalloy is due to the change of growth mode of the γ′ phase during isothermal aging in the 2Cr superalloy.

In this work, the diffusion coefficient (D_1) of Cr and Mo in FCC-Co are calculated by the Arrhenius equation (Lapin et al., 2008; Yuan et al., 2019):

$$D_1 = D_0 e^{-\frac{Q}{RT}} \tag{4}$$

Where D_0 represents the frequency factor, Q represents the diffusion activation energy, R represents the ideal gas constant [8.314 J/(K·mol)], and T represents the absolute temperature (1073 K). The values of D_0 and Q are obtained from references (Neumeier et al., 2016), and some parameters and D_1 values are listed in **Table 3**.

The diffusion coefficient of Cr is slightly larger than that of Mo, which means Cr diffuses faster than Mo in FCC-Co, and Mo prefers to be distributed in the γ′ phase to Cr, so Mo takes a longer time to reach steady-state diffusion in whole system. Therefore, the 2Cr superalloy reached steady-state diffusion earlier than the 2Mo superalloy, and the γ′ phase in the 2Cr superalloy grows faster by merging with each other. The merger between γ′ phases was observed by TEM at an early aging stage, as shown in **Figure 9A** (the red circle in the micrograph). Hence, it can be speculated that the coarsening rate of the 2Cr superalloy is obviously higher than that of

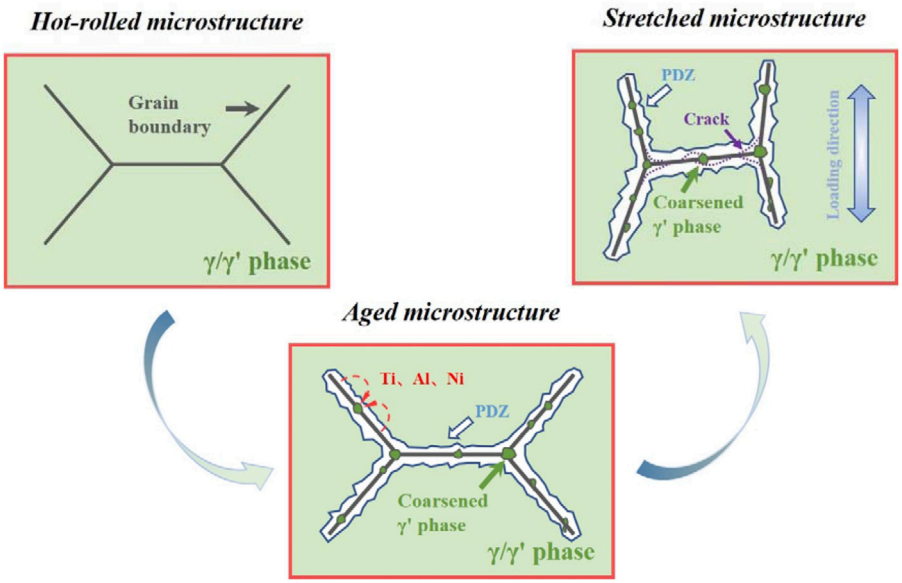

FIGURE 12 | Schematic diagram of microstructure evolution during isothermal aging stretching.

the 2Mo superalloy. In a later isothermal aging period, due to the coarsening of the 2Cr superalloy being limited by the interfacial reaction, that of the 2Mo superalloy is still limited by the diffusion of atoms, so the size of the γ′ phase in the 2Cr superalloy is larger than that of the 2Mo superalloy (Li et al., 2018; Ng et al., 2020). When the coarsening of the γ′ phase is limited by interfacial reaction, the driving force of the γ′ phase coarsening is the decrease of interfacial energy (*i.e.*, the decrease of the interfacial area by merging between a few γ′ phases). The coarsening rate is obviously higher than that of the γ′ phase coarsening caused by solute atom diffusion.

Failure Mechanism

The yield strength of 2Cr and 2Mo superalloys after being aged for 16 h at 1073 K is 755 and 909 MPa respectively, which is higher than Co-Al-Mo-Nb-based superalloys and Co-Ni-Mo-Al-Ta-based superalloys reported by Makineni et al. (2015a); Makineni et al. (2015b) Meanwhile, the yield strength also exceeds that of traditional Co-based superalloys (MAR-M-302, HAYNES-188), and the yield strength of the 2Mo superalloy is higher than that of Ni-based superalloys (WASPALOY, MAR-M-247) (Makineni et al., 2015b). Micrographs of two Co-Ni-Al-Ti-based superalloys after isothermal aging at 1073 K are shown in **Figure 10**. During the isothermal aging process, the strength of superalloys gradually decreases, but no harmful phases are observed in the micrographs. Therefore, it is confirmed that the coarsening of the γ′ phase is the main reason for the reduction of strength, especially the γ′ phase at the grain boundary. The coarsening of the γ′ phase leads to a widened channel of the γ phase, which causes dislocations to slip more easily and reduces the strength of the superalloys. Besides, defects (grain boundaries, dislocation, etc.) can accelerate element diffusion in superalloys. In addition, PDZ was formed near the grain boundary due to migration of the γ′ phase forming elements to the coarsening γ′ phase at the grain boundary, and further weakens grain boundaries (Zhang et al., 2018). In the meantime, consumption of alloying elements will reduce the solution strengthening effect in the matrix. The side-view micrographs of superalloy tensile test samples are shown in **Figure 11**. Under action of stress, the grain boundary becomes the location for nucleation and growth of cracks. Applied stress deforms the grain along the loading direction and cracks appear at the grain boundary along the vertical loading direction. Besides, the coarsened γ′ phase in the grain boundary is observed at the fracture edge, which proves that cracks propagate along the grain boundary, and grain boundaries possess a lower strength and higher brittleness as compared to that of inner grains (George et al., 1995).

A schematic diagram of microstructure evolution during isothermal aging stretching is shown in **Figure 12**. The elements forming the γ′ phase near the grain boundary diffuse towards the grain boundary during the isothermal aging process, resulting in the coarsening of the γ′ phase on the grain boundary. Meanwhile, the lack of γ′ forming elements leads to the formation of PDZ near grain boundary, which weakens precipitation strengthening and solution strengthening near grain boundaries. Under action of stress, the grain boundary becomes the weakest part of superalloys, cracks nucleate and grow near the grain boundary in the direction of the vertical load, and finally lead to the fracture of the sample. In conclusion, the failure mechanism of 2Cr and 2Mo superalloys is still a plastic fracture mechanism, but the grain boundary becomes the worst mechanical position due to the coarsening of the γ′ phase at the grain boundaries and the formation of PDZ around the grain boundaries.

CONCLUSION

In this study, microstructure evolution and mechanical performances of Co-Ni-Al-Ti-based superalloys after

isothermal aging at 1073 K were studied, and the following conclusions were obtained:

1) The temporal exponents of 2Cr and 2Mo superalloys are 2.17 ± 0.3 and 2.78 ± 0.24 respectively. The iffusion rate of Cr atoms in FCC-Co is faster and the diffusion distance is shorter, which leads to the coarsening of 2Cr superalloys reaching the second stage in advance. Hence, especially in the later aging stage, the coarsening rate of the 2Cr superalloy is obviously higher than that of the 2Mo alloy.
2) In the isothermal aging process, the coarsening of the γ′ phase at the grain boundary consumes alloying elements in the surrounding γ′ phase and matrix, which weakens the matrix and grain boundary. Complex interfaces and the high energy of the grain boundary are favorable to nucleation and propagation of cracks.
3) Compared with the 2Cr superalloy, the 2Mo superalloy has more excellent mechanical properties because Mo elements prefer distribution in the γ′ phase, which increases the volume fraction of the γ′ phase. Meanwhile, Mo has a stronger solution strengthening effect in the γ phase matrix.
4) Mechanical properties of the 2Cr and 2Mo superalloys decrease with isothermal aging time, which is caused by the coarsening of the γ′ phase. In addition, the higher coarsening rate of the γ′ phase results in mechanical properties decreasing more significantly in the 2Cr superalloy.

DATA AVAILABILITY STATEMENT

The raw data supporting the conclusion of this article will be made available by the authors, without undue reservation.

ETHICS STATEMENT

Written informed consent was obtained from the individual(s) for the publication of any potentially identifiable images or data included in this article.

AUTHOR CONTRIBUTIONS

XZ: Conceptualization, Data curation, Formal analysis, Investigation, Software, Writing-original draft, Writing-review and editing. HS: Conceptualization, Data curation, Formal analysis, Investigation, Software, Writing-original draft. QG: Conceptualization, Data curation, Formal analysis, Funding acquisition, Investigation, Methodology, Project administration, Supervision, Validation, Writing-review and editing. QM: Conceptualization, Data curation, Formal analysis, Investigation. HZ: Conceptualization, Data curation, Formal analysis, Investigation, Methodology, Writing-review and editing. HL: Conceptualization, Formal analysis, Funding acquisition, Supervision. LS: Formal analysis, Software, Validation.

FUNDING

The grants and financial supports from the National Natural Science Foundation of China (Grant Nos. 52171107, 51871042), the National Natural Science Foundation of China-Joint Fund of Iron and Steel Research (Grant No. U1960204) and the Fundamental Research Funds for the Central Universities (Grant No. N2123010) are gratefully acknowledged.

REFERENCES

Azzam, A., Philippe, T., Hauet, A., Danoix, F., Locq, D., Caron, P., et al. (2018). Kinetics Pathway of Precipitation in Model Co-Al-W Superalloy. *Acta. Mat.* 145, 377–387. doi:10.1016/j.actamat.2017.12.032

Chen, J., Guo, M., Yang, M., Su, H., Liu, L., and Zhang, J. (2021a). Phase-Field Simulation of γ′ Coarsening Behavior in Cobalt-Based Superalloy. *Comp. Mat. Sci.* 191, 110358. doi:10.1016/j.commatsci.2021.110358

Chen, Y., Wang, C., Ruan, J., Yang, S., Omori, T., Kainuma, R., et al. (2020). Development of Low-Density γ/γ′ Co-Al-Ta-Based Superalloys with High Solvus Temperature. *Acta. Mat.* 188, 652–664. doi:10.1016/j.actamat.2020.02.049

Chen, Y., Xue, F., Wang, C., Li, X., Deng, Q., Yang, X., et al. (2019). Effect of Cr on the Microstructure and Oxidation Properties of Co-Al-W Superalloys Studied by *In Situ* Environmental TEM. *Corros. Sci.* 161, 108179. doi:10.1016/j.corsci.2019.108179

Chen, Z., Okamoto, N. L., Chikugo, K., and Inui, H. (2021b). On the Possibility of Simultaneously Achieving Sufficient Oxidation Resistance and Creep Property at High Temperatures Exceeding 1000 °C in Co-Based Superalloys. *J. Alloy. Compd.* 858, 157724. doi:10.1016/j.jallcom.2020.157724

Chung, D.-W., Toinin, J. P., Lass, E. A., Seidman, D. N., and Dunand, D. C. (2020). Effects of Cr on the Properties of Multicomponent Cobalt-Based Superalloys with Ultra High γ' Volume Fraction. *J. Alloy. Compd.* 832, 154790. doi:10.1016/j.jallcom.2020.154790

Feng, K., Li, M., Chen, M., Li, Z., Sha, J., and Zhou, C. (2021). Cyclic Oxidation Behavior of Al-Si Coating on New γ′-Strengthened Cobalt-Based Superalloy: Experimental Study and First-Principles Calculation. *Corros. Sci.* 185, 109422. doi:10.1016/j.corsci.2021.109422

Gao, Q., Jiang, C., Zhang, H., Ma, Q., Zhang, H., Liu, Z., et al. (2022). Co-Strengthening of Dislocations and Precipitates in Alumina-Forming Austenitic Steel with Cold Rolling Followed by Aging. *Mater. Sci. Eng. A* 831, 142181. doi:10.1016/j.msea.2021.142181

Gao, Q., Jiang, Y., Liu, Z., Zhang, H., Jiang, C., Zhang, X., et al. (2020). Effects of Alloying Elements on Microstructure and Mechanical Properties of Co-Ni-Al-Ti Superalloy. *Mater. Sci. Eng. A* 779, 139139. doi:10.1016/j.msea.2020.139139

Gao, Q., Liu, Z., Li, H., Zhang, H., Jiang, C., Hao, A., et al. (2021a). High-Temperature Oxidation Behavior of Modified 4Al Alumina-Forming Austenitic Steel: Effect of Cold Rolling. *J. Mat. Sci. Technol.* 68, 91–102. doi:10.1016/j.jmst.2020.08.013

Gao, Q., Lu, B., Ma, Q., Zhang, H., Li, H., and Liu, Z. (2021b). Effect of Cu Addition on Microstructure and Properties of Fe-20Ni-14Cr Alumina-Forming Austenitic Steel. *Intermetallics* 138, 107312. doi:10.1016/j.intermet.2021.107312

Gao, Q., Shang, H., Ma, Q., Zhang, H., Zhang, H., Li, H., et al. (2021c). Isothermal Oxidation Behavior of W-Free Co-Ni-Al-Based Superalloy at High Temperature. *Mat. Corros.* 73, 513–525. doi:10.1002/maco.202112789

George, E. P., Liu, C. T., Lin, H., and Pope, D. P. (1995). Environmental Embrittlement and Other Causes of Brittle Grain Boundary Fracture in Ni3Al. *Mater. Sci. Eng. A* 192-193, 277–288. doi:10.1016/0921-5093(94)03236-x

Guan, Y., Liu, Y., Ma, Z., Li, H., and Yu, H. (2022). Effect of Microstructure on Temperature Dependence of Deformation Behavior in Polycrystalline CoNi-Based Superalloy. *J. Mat. Sci.* 57 (1), 687–699. doi:10.1007/s10853-021-06582-x

Guan, Y., Liu, Y., Ma, Z., Li, H., and Yu, H. (2020a). Investigation on γ′ Stability in CoNi-Based Superalloys during Long-Term Aging at 900 °C. *J. Alloy. Compd.* 842, 155891. doi:10.1016/j.jallcom.2020.155891

Guan, Y., Liu, Y., Ma, Z., Li, H., and Yu, H. (2020b). Precipitation and Coarsening Behavior of γ′ Phase in CoNi-Base Superalloy under Different Aging Treatments. *Vacuum* 175, 109247. doi:10.1016/j.vacuum.2020.109247

Jiang, J., Liu, Z., Gao, Q., Zhang, H., Hao, A., Qu, F., et al. (2020). The Effect of Isothermal Aging on Creep Behavior of Modified 2.5Al Alumina-Forming Austenitic Steel. *Mater. Sci. Eng. A* 797, 140219. doi:10.1016/j.msea.2020.140219

Jiang, Y., Gao, Q., Zhang, H., Zhang, X., Li, H., Liu, Z., et al. (2019). The Effect of Isothermal Aging on Microstructure and Mechanical Behavior of Modified 2.5Al Alumina-Forming Austenitic Steel. *Mater. Sci. Eng. A* 748, 161–172. doi:10.1016/j.msea.2019.01.087

Lapin, J., Gebura, M., Pelachová, T., and Nazmy, M. (2008). Coarsening Kinetics of Cuboidal Gamma Prime Precipitates in Single Crystal Nickel Base Superalloy CMSX-4. *Kov. Mater.* 46, 313–322.

Li, C., Chung, D.-W., Dunand, D. C., and Seidman, D. N. (2020a). Microstructural Stability and Mechanical Behavior of a Co–20Ni–7Al–7W–4Ti at.% Superalloy. *J. Alloy. Compd.* 848, 156378. doi:10.1016/j.jallcom.2020.156378

Li, W., Li, L., Antonov, S., Lu, F., and Feng, Q. (2020b). Effects of Cr and Al/W Ratio on the Microstructural Stability, Oxidation Property and γ′ Phase Nano-Hardness of Multi-Component Co-Ni-Base Superalloys. *J. Alloys Compd.* 826, 154182. doi:10.1016/j.jallcom.2020.154182

Li, Y., Pyczak, F., Paul, J., Oehring, M., Lorenz, U., Yao, Z., et al. (2018). Rafting of γ′ Precipitates in a Co-9Al-9W Superalloy during Compressive Creep. *Mater. Sci. Eng. A* 719, 43–48. doi:10.1016/j.msea.2018.02.017

Liu, J., Yu, J. J., Yang, Y. H., Zhou, Y. Z., and Sun, X. F. (2019). Effects of Mo on the Evolution of Microstructures and Mechanical Properties in Co-Al-W Base Superalloys. *Mater. Sci. Eng. A* 745, 404–410. doi:10.1016/j.msea.2018.11.087

Lu, S., Antonov, S., Xue, F., Li, L., and Feng, Q. (2021). Segregation-Assisted Phase Transformation and Anti-Phase Boundary Formation during Creep of a γ′-strengthened Co-Based Superalloy at High Temperatures. *Acta Mater.* 215, 117099. doi:10.1016/j.actamat.2021.117099

Makineni, S. K., Nithin, B., and Chattopadhyay, K. (2015a). A New Tungsten-Free γ-γ' Co-al-Mo-Nb-Based Superalloy. *Scr. Mat.* 98, 36–39. doi:10.1016/j.scriptamat.2014.11.009

Makineni, S. K., Samanta, A., Rojhirunsakool, T., Alam, T., Nithin, B., Singh, A. K., et al. (2015b). A New Class of High Strength High Temperature Cobalt Based γ-γ′ Co-Mo-Al Alloys Stabilized with Ta Addition. *Acta. Mat.* 97, 29–40. doi:10.1016/j.actamat.2015.06.034

Mukherji, D., Gilles, R., Barbier, B., Genovese, D. D., and Rösler, J. (2003). Lattice Misfit Measurement in Inconel 706 Containing Coherent γ′ and γ″ Precipitates. *Scr. Mat.* 48 (4), 333–339. doi:10.1016/S1359-6462(02)00456-6

Neumeier, S., Rehman, H. U., Neuner, J., Zenk, C. H., Michel, S., Schuwalow, S., et al. (2016). Diffusion of Solutes in Fcc Cobalt Investigated by Diffusion Couples and First Principles Kinetic Monte Carlo. *Acta. Mat.* 106, 304–312. doi:10.1016/j.actamat.2016.01.028

Ng, D. S., Chung, D.-W., Toinin, J. P., Seidman, D. N., Dunand, D. C., and Lass, E. A. (2020). Effect of Cr Additions on a γ-γ' Microstructure and Creep Behavior of a Co-Based Superalloy with Low W Content. *Mater. Sci. Eng. A* 778, 139108. doi:10.1016/j.msea.2020.139108

Omori, T., Sutou, Y., Oikawa, K., Kainuma, R., and Ishida, K. (2006). Shape Memory and Magnetic Properties of Co-Al Ferromagnetic Shape Memory Alloys. *Mater. Sci. Eng. A* 438-440, 1045–1049. doi:10.1016/j.msea.2005.12.068

Pandey, P., Raj, A., Baler, N., and Chattopadhyay, K. (2021). On the Effect of Ti Addition on Microstructural Evolution, Precipitate Coarsening Kinetics and Mechanical Properties in a Co-30Ni-10Al-5Mo-2Nb Alloy. *Materialia* 16, 101072. doi:10.1016/j.mtla.2021.101072

Sato, J., Omori, T., Oikawa, K., Ohnuma, I., Kainuma, R., and Ishida, K. (2006). Cobalt-Base High-Temperature Alloys. *Science* 312 (5770), 90–91. doi:10.1126/science.1121738

Sauza, D. J., Dunand, D. C., Noebe, R. D., and Seidman, D. N. (2019a). γ'-(L12) Precipitate Evolution during Isothermal Aging of a Co Al W Ni Superalloy. *Acta. Mat.* 164, 654–662. doi:10.1016/j.actamat.2018.11.014

Sauza, D. J., Dunand, D. C., and Seidman, D. N. (2019b). Microstructural Evolution and High-Temperature Strength of a γ(f.c.c.)/γ'(L12) Co-Al-W-Ti-B Superalloy. *Acta. Mat.* 174, 427–438. doi:10.1016/j.actamat.2019.05.058

Singh, M. P., Olu, E. F., Pandey, P., and Chattopadhyay, K. (2021). Thermophysical and Magnetic Properties of Co-Ni-Mo-Al-Ta Class of Tungsten Free Co-Based Superalloys. *J. Alloy. Compd.* 879, 160379. doi:10.1016/j.jallcom.2021.160379

Wang, C., Li, K., Han, J., Chen, Y., Chen, Y., Wang, Y., et al. (2019). Temperature Dependence of Thermodynamic Stability and Mechanical Property of Alloying Co3Ta Compounds. *J. Alloy. Compd.* 808, 151068. doi:10.1016/j.jallcom.2019.06.170

Wen, M., Sun, Y., Yu, J., Yang, Y., Zhou, Y., and Sun, X. (2020). Effects of Al Content on Microstructures and High-Temperature Tensile Properties of Two Newly Designed CoNi-Base Superalloys. *J. Alloy. Compd.* 835, 155337. doi:10.1016/j.jallcom.2020.155337

Xu, W.-W., Xiong, Z. Y., Gong, X. G., Yin, G. H., Chen, L. J., Wang, C. P., et al. (2021a). Accelerating the Discovery of Novel γ/γ' Co-Based Superalloys by Probing Temperature and Alloying Effects on the γ' Precipitates. *Materialia* 18, 101171. doi:10.1016/j.mtla.2021.101171

Xu, W.-W., Yin, G. H., Xiong, Z. Y., Yu, Q., Gang, T. Q., and Chen, L. J. (2021b). Plasticity-Induced Stacking Fault Behaviors of γ' Precipitates in Novel CoNi-Based Superalloys. *J. Mat. Sci. Technol.* 90, 20–29. doi:10.1016/j.jmst.2021.02.031

Yoo, B., Im, H. J., Seol, J.-B., and Choi, P.-P. (2019). On the Microstructural Evolution and Partitioning Behavior of L12-Structured γ′-Based Co-Ti-W Alloys upon Cr and Al Alloying. *Intermetallics* 104, 97–102. doi:10.1016/j.intermet.2018.10.027

Yuan, Y., Chen, T., Li, D., Gerhards, U., Pan, F., Seifert, H., et al. (2019). Diffusion Multiple Study of the Co-Fe-Ni System at 800 °C. *Calphad* 64, 149–159. doi:10.1016/j.calphad.2018.12.005

Zenk, C. H., Neumeier, S., Stone, H. J., and Göken, M. (2014). Mechanical Properties and Lattice Misfit of γ/γ′ Strengthened Co-base Superalloys in the Co-W-Al-Ti Quaternary System. *Intermetallics* 55, 28–39. doi:10.1016/j.intermet.2014.07.006

Zenk, C. H., Povstugar, I., Li, R., Rinaldi, F., Neumeier, S., Raabe, D., et al. (2017). A Novel Type of Co-Ti-Cr-base γ/γ′ Superalloys with Low Mass Density. *Acta. Mat.* 135, 244–251. doi:10.1016/j.actamat.2017.06.024

Zhang, Y., Fu, H., Zhou, X., Zhang, Y., Dong, H., and Xie, J. (2020). Microstructure Evolution of Multicomponent γ′-Strengthened Co-Based Superalloy at 750 °C and 1000 °C with Different Al and Ti Contents. *Metall. Mat. Trans. A* 51 (4), 1755–1770. doi:10.1007/s11661-020-05652-0

Zhang, Y., Fu, H., Zhou, X., Zhang, Y., and Xie, J. (2018). Effects of Aluminum and Molybdenum Content on the Microstructure and Properties of Multi-Component γ′-Strengthened Cobalt-Base Superalloys. *Mater. Sci. Eng. A* 737, 265–273. doi:10.1016/j.msea.2018.09.058

Zhou, H. J., Xue, F., Chang, H., and Feng, Q. (2018). Effect of Mo on Microstructural Characteristics and Coarsening Kinetics of γ' Precipitates in Co-Al-W-Ta-Ti Alloys. *J. Mat. Sci. Technol.* 34 (5), 799–805. doi:10.1016/j.jmst.2017.04.012

Zhou, X., Fu, H., Xue, F., Zhang, Y., and Xie, J. (2020). Abnormal Precipitation of the μ Phase during Solution Treatment of γ′-strengthened Co-Ni-Al-W-Based Superalloys. *Scr. Mater* 181, 30–34. doi:10.1016/j.scriptamat.2020.02.010

Zhuang, X., Lu, S., Li, L., and Feng, Q. (2020). Microstructures and Properties of a Novel γ′-strengthened Multi-Component CoNi-Based Wrought Superalloy Designed by CALPHAD Method. *Mater. Sci. Eng. A* 780, 139219. doi:10.1016/j.msea.2020.139219

Conflict of Interest: Author HZ was employed by the company Daotian High Technology Co., Ltd.

The remaining authors declare that the research was conducted in the absence of any commercial or financial relationships that could be construed as a potential conflict of interest.

Publisher's Note: All claims expressed in this article are solely those of the authors and do not necessarily represent those of their affiliated organizations, or those of the publisher, the editors and the reviewers. Any product that may be evaluated in this article, or claim that may be made by its manufacturer, is not guaranteed or endorsed by the publisher.